Peptidoglycan-Chi3l1 interaction shapes gut microbiota in intestinal mucus layer

Yan Chen[1#], Ruizhi Yang[1#], Bin Qi[1]*, Zhao Shan[1]*

Southwest United Graduate School, Yunnan Key Laboratory of Cell Metabolism and Diseases, State Key Laboratory of Conservation and Utilization of Bio-resources in Yunnan, Center for Life Sciences, School of Life Sciences, Yunnan University, Kunming, China, 650500*Corresponding author

*email: Bin Qi: qb@ynu.edu.cn and Zhao Shan: shanzhao@ynu.edu.cn
# Equally contributed

Abstract

The balanced gut microbiota in intestinal mucus layer plays an instrumental role in the health of the host. However, the mechanisms by which the host regulates microbial communities in the mucus layer remain largely unknown. Here, we discovered that the host regulates bacterial colonization in the gut mucus layer by producing a protein called Chitinase 3-like protein 1 (Chi3l1). Intestinal epithelial cells are stimulated by the gut microbiota to express Chi3l1. Once expressed, Chi3l1 is secreted into the mucus layer where it interacts with the gut microbiota, specifically through a component of bacterial cell walls called peptidoglycan. This interaction between Chi3l1 and bacteria is beneficial for the colonization of bacteria in the mucus, particularly for gram-positive bacteria like *Lactobacillus*. Moreover, a deficiency of Chi3l1 leads to an imbalance in the gut microbiota, which exacerbates colitis induced by dextran sodium sulfate (DSS). By performing fecal microbiota transplantation from Villin-cre mice or replenishing *Lactobacillus* in IEC$^{\Delta Chil1}$ mice, we were able to restore their colitis to the same level as that of Villin-cre mice. In summary, this study shows a "scaffold model" for microbiota homeostasis by interaction between intestinal Chi3l1 and bacteria cell wall interaction, and it also highlights that an unbalanced gut microbiota in the intestinal mucus contributes to the development of colitis.

Key words: Chi3l1, intestinal homeostasis, gut microbiota, peptidoglycan,

Introduction

Intestinal homeostasis is crucial for maintaining human health[1]. Alterations in gut microbiota composition have been linked to various diseases including cancer, obesity, and neurological disorders[2-6]. Dysbiosis, which refers to an imbalance in gut microbiota, is characterized by decreased microbial diversity, the presence of harmful microbes, or absence of beneficial ones [7]. Therefore, understanding the factors that influence gut microbiota is a fundamental goal in microbiome research[8]. Growing evidence suggests that colonization of the gut mucus layer can affect the susceptibility and progression of intestinal diseases like inflammatory bowel disease (IBD), irritable bowel syndrome, and celiac disease[9]. Inflammatory bowel diseases, such as Crohn's disease (CD) and Ulcerative Colitis (UC), are characterized by chronic inflammation of

the intestinal mucosa. Although the cause of the inflammatory bowel disease is unclear, mouse models lacking the key components of the mucus are predisposed to colitis, accompanied by dysbiosis in mucosa[10, 11], which is in accordance with increased epithelial-adherent microbial communities in biopsies from patients with IBD [12, 13]. Furthermore, there were significant differences in the gut microbiota of CD patients compared with healthy controls, and these differences were only present in mucus samples (not stool samples), suggesting that bacteria in the mucus layer may be more important for the development of IBD[14]. Donaldson et al. discovered that the intestinal flora utilizes host immunoglobulin A (IgA) for mucus colonization, indicating that the host may secrete certain factors to maintain intestinal flora homeostasis in the mucus[15]. However, the mechanisms regulating gut microbiota colonization in the mucus layer remain largely unknown. We aim to investigate the regulation of microbial communities in gut mucus and its implications in intestinal diseases.

Chitinase 3-like protein 1 (Chi3l1, also known as YKL-40 in humans) is a secreted protein that belongs to the glycosylhydrolase 18 family[16]. Despite its name, Chi3l1 can bind to chitin but does not have chitinase activity[17]. In our investigation, we noticed that chitin and peptidoglycan, a major component of bacterial cell walls, have similar structures [18]. Based on this information, we speculate that Chi3l1 might also interact with peptidoglycan and, therefore, interact with bacteria. Interestingly, Chi3l1 is expressed in intestinal epithelial cells and the lamina propria. We hypothesize that Chi3l1 may be secreted by intestinal epithelial cells and regulate the gut microbiota through its interaction with peptidoglycan in the mucous layer. In our study, we discovered that gut microbiota induce the expression of Chi3l1 in epithelial cells. Once expressed, Chi3l1 is secreted into the mucosa and interacts with bacteria, particularly with the bacterial cell wall component peptidoglycan. This interaction promotes bacterial colonization, especially of beneficial bacteria such as *Lactobacillus*. As a result, mice with higher levels of Chi3l1 are less susceptible to colitis.

Results

Intestinal epithelial cells express Chi3l1 induced by gut microbiota.

The gut microbiota's composition is shaped by host factors, including IgA [15], RegIIIγ [19], and TLR-5 [18]. Yet, specific host factors which maintain the homeostasis of the microbiota remain largely undefined. Drawing on the theory of co-evolution between the host and microbiota [20], we propose that host factors, which are induced by bacteria in the gut, could play a pivotal role in regulating bacterial colonization and composition. In a previous study, it was observed that both live *E.coli* and heat-killed *E.coli* treatment resulted in a significant increase in the expression of the gene encoding Chi3l1 in human intestinal organoids[21]. To verify this finding, we conducted immunohistochemical staining on intestinal tissue sections of germ-free and specific pathogen free (SPF) C57BL/6J wildtype mice. We observed a substantial increase of Chi3l1 expression in SPF mice compared to germ-free mice (Fig. 1A). The intestinal epithelium comprises various cell types, including intestinal cells, goblet cells, endoentercrine cells, Tuft cells, Paneth cells, M cells, and others [21]. To identify the cellular sources of Chi3l1, we performed co-staining with markers for specific cell types, including Chromogranin A (ChgA) for enteroendocrine cells, Ulex

Europaeus Agglutinin I (UEA-1) for goblet cells and Paneth cells, and Double cortin-like kinase 1 (DCLK1) for tuft cells. Our results revealed that Chi3l1 is primarily expressed in enteroendocrine cells in the ileum and goblet or Paneth cells in the colon (Fig. 1B). However, Chi3l1 expression was not observed in tuft cells (Supplementary Figure 1).

Furthermore, we isolated total bacteria from wildtype mouse feces and treated DLD-1 cells (a colorectal adenocarcinoma cell line) with the bacterial extract for 12 hours. We found that the bacterial extract directly induced Chi3l1 expression in DLD-1 cells (Fig. 1C). To examine whether the induction of Chi3l1 expression require a specific bacteria strain, we further identified the bacterial extract using 16S rRNA sequencing. Our results revealed that *E.coli* specifically stimulated Chi3l1 expression in DLD-1 cells, while *Staphylococcus Sciuri* did not have the same effect (Fig. 1D). Although our data are limited to these two bacterial strains, it suggest that not all bacteria can induce the expression of Chi3l1. Next, we wondered what component of bacteria can induce Chi3l1 expression. We tried heat-killed *E.coli*, which maintains bacterial cell wall integrity. We found that treatment of DLD-1 cells with heat-killed *E.coli* also led to an induction of Chi3l1 expression (Fig. 1E). These findings suggest that the induction of Chi3l1 expression does not necessarily require live bacteria and that bacterial components alone are sufficient to induce this response.

Given that *E. coli* is Gram-negative and *Staphylococcus sciuri* is Gram-positive, we hypothesized that the difference in their ability to induce Chi3l1 expression might be due to variations between Gram-negative and Gram-positive bacteria, such as the presence of lipopolysaccharides (LPS). To test this hypothesis, we used LPS to induce Chi3l1 expression. Consistent with our hypothesis, LPS successfully induced Chi3l1 expression (Fig. 1F&G). Collectively, these findings provide evidence that the gut microbiota can induce Chi3l1 expression in intestinal epithelial cells. Collectively, these findings provide evidence that the gut microbiota can induce Chi3l1 expression in intestinal epithelial cells.

Chi3l1 interact with bacteria via peptidoglycan.

Chi3l1 belongs to a group of proteins called non-enzymatic chitinase-like proteins, which are known to bind chitin. Chitin is a polysaccharide present in the exoskeleton of arthropods and the cell walls of fungi[22]. By comparing the structure of chitin with that of peptidoglycan (PGN), a component of bacterial cell walls, we observed that they have similar structures (Fig. 2A). Based on this observation, we hypothesized that Chi3l1 may interact with gut bacteria through PGN. To test our hypothesis, we conducted co-incubation experiments where we mixed recombinant mouse Chi3l1 (rmChi3l1) with either Gram-positive or Gram-negative bacteria and then precipitated the bacteria through centrifugation. We found that rmChi3l1 was present in the pellet obtained from both Gram-positive and Gram-negative bacteria (Fig. 2B), suggesting that Chi3l1 can directly interact with bacteria.

To further investigate the interaction between Chi3l1 and PGN, we also co-incubated PGN with rmChi3l1 and precipitated the PGN through centrifugation. PGN is an insoluble substance and hence can be precipitated by centrifugation. Consistent with our previous results, we observed that

rmChi3l1 was present in the pellet obtained from PGN but not in the pellet obtained from bovine serum albumin (BSA), which served as a negative control (Fig. 2C). Furthermore, we also examined the interaction between PGN and recombinant human Chi3l1 (rhChi3l1) and obtained similar results (Fig. 2D). These findings indicate that Chi3l1 interacts with bacteria through PGN.

To better characterize the binding between Chi3l1 and peptidoglycan (PGN), we compared the binding affinities of Chi3l1 to both PGN and chitin. We incubated chitin and PGN with rmChi3l1 in increasing doses (25, 50, 100 μg) and detected the precipitated rmChi3l1 by either chitin or PGN. Our results indicate that Chi3l1 interacts with PGN in a dose-dependent manner (Figure 2E). In contrast, the binding between Chi3l1 and chitin did not exhibit dose dependency (Figure 2E). These findings suggest a specific and distinct binding mechanism for Chi3l1 with PGN compared to chitin.

To investigate whether the Chi3l1-PGN interaction could facilitate the colonization of gram-positive bacteria, we conducted adhesion experiments using DLD-1 cells and bacteria. We employed a GlmM mutant (PGN synthesis-deficient) and K12 bacteria (a wild-type E. coli strain used as a control) to assess their adhesion capabilities. The results showed that the adhesion ability of the GlmM mutant to cells significantly decreased (Figure 2F). Additionally, after knocking down Chi3l1 in DLD-1 cells (knockdown efficiency over 50%), we observed a decrease in bacterial adhesion (Figure 2G). These findings suggest that the Chi3l1-PGN interaction plays a crucial role in bacterial adhesion.

Intestinal bacteria are disordered in IEC$^{\Delta Chil1}$ mice, especially Gram-positive bacteria.

To gain initial insights into how the expression of Chi3l1 in intestinal epithelial cells (IECs) affects the colonization of gut microbiota, we created mice with a specific deficiency of Chi3l1 in IECs (referred to as IEC$^{\Delta Chil1}$ mice) (Supplementary Figure 2). We then conducted bacterial 16S rRNA sequencing analysis of the colon contents of both Villin-cre and IEC$^{\Delta Chil1}$ littermates. Our analysis of alpha diversity revealed that the bacterial population was relatively lower in IEC$^{\Delta Chil1}$ littermates compared to Villin-cre littermates (Figure 3A). This finding was further confirmed by conducting universal bacterial 16S rRNA qPCR analysis of the feces and ileum contents of IEC$^{\Delta Chil1}$ and Villin-cre littermates, which also showed lower bacterial enrichment in IEC$^{\Delta Chil1}$ mice (Figure 3B). Furthermore, principal component analysis demonstrated significant differences in bacterial diversity between Villin-cre and IEC$^{\Delta Chil1}$ littermates (Figure 3C).

When we examined the relative abundance of Gram-positive and Gram-negative bacteria between Villin-cre and IEC$^{\Delta Chil1}$ littermates, we observed that Gram-positive bacteria were significantly reduced in IEC$^{\Delta Chil1}$ mice, while there was no notable difference in Gram-negative bacteria (Figure 3D). This result was further validated by staining lipoteichoic acid (LTA), a component present on Gram-positive bacteria, which revealed a lower abundance of Gram-positive bacteria in IEC$^{\Delta Chil1}$ compared to Villin-cre littermates (Figure 3E). Moreover, visualization of *Firmicutes* by bacteria FISH staining, a dominant group of Gram-positive bacteria in the gut, also showed reduced levels of *Firmicutes* in the colon lumen of IEC$^{\Delta Chil1}$ mice compared to Villin-cre mice (Figure 3F). Analysis of the relative abundance of specific Gram-positive bacterial species demonstrated a

177 significant reduction in *Lactobacillus* in IEC$^{\Delta Chil1}$ mice compared to Villin-cre mice (Figure 3G).
178 Similar results were observed in Chil1$^{-/-}$ mice compared to wildtype mice (Figure 3H). Consist
179 with the 16S rRNA sequencing analysis data, qPCR results showed that *Turicibacter* was more
180 abundant in IEC$^{\Delta Chil1}$ mice than Villin-cre mice (Supplementary Figure 3A). These findings
181 suggest that Chi3l1 plays a role in regulating the colonization of Gram-positive bacteria,
182 particularly *Lactobacillus*, in the murine gut.
183
184 **Chi3l1 promotes the colonization of Gram-positive bacteria in intestinal mucus.**
185
186 Chi3l1 was found in secretory cells like goblet cells and Paneth cells, suggesting that it may be
187 secreted into the intestinal lumen (Fig. 1B). Immunohistochemistry staining of Chi3l1 in the colon
188 revealed a large amount of Chi3l1 signals in the mucus layer (Fig. 4A). Immunofluorescence co-
189 staining of Chi3l1 with UEA-1 in the colon yielded similar results (Fig. 4B). Furthermore, Chi3l1
190 was also detected in the ileum and colonic tissues and mucus layer (Fig. 4C&D). These findings
191 indicate that mouse Chi3l1 is specifically expressed in intestinal secretory epithelial cells and
192 secreted into the intestinal lumen. Since large amounts of Chi3l1 is secreted into the mucus and
193 Chi3l1 interact with bacteria, we hypothesize that Chi3l1 may regulate the colonization of Gram-
194 positive bacteria in the mucus layer. To test this hypothesis, we isolated bacterial DNA from the
195 ileum and colon mucus of both wildtype and Chi1l1$^{-/-}$ mice. Quantification of Gram-positive
196 bacteria and *Lactobacillus* using qPCR revealed that both the ileum and colon mucus of Chi1l1$^{-/-}$
197 mice had significantly lower levels of Gram-positive bacteria and *Lactobacillus* compared to that
198 of wildtype mice (Fig. 4E&F).
199
200 To further validate these results, we labeled a Gram-positive bacteria strain, *E. faecalis*, with
201 fluorescent D-amino acids (FDAA), which can metabolically label bacterial peptidoglycans[23].
202 We then performed rectal injection of both wildtype and Chi1l1$^{-/-}$ mice with FDAA-labeled *E.*
203 *faecalis*. The data demonstrated that Chi1l1$^{-/-}$ mice had much lower colonization of *E. faecalis*
204 compared to wildtype mice (Fig. 4G). Besides Gram-positive bacteria, we also performed rectal
205 injection of both wildtype and Chi1l1$^{-/-}$ mice with mCherry-OP50 (*a strain of E.coli that express*
206 *mCherry*), we found Chi1l1$^{-/-}$ mice had much higher colonization of *E. coli* compared to wildtype
207 mice (Supplementary Figure 3B). Based on these findings, we conclude that Chi3l1 promotes the
208 colonization of Gram-positive bacteria, particularly *Lactobacillus*, in the intestinal mucus.
209 Additionally, we also observed that the deletion of Chi3l1 significantly reduced mucus layer
210 thickness, which may be attributed to the disrupted colonization of Gram-positive bacteria in the
211 intestinal mucus layer (Supplementary Figure 3 A&B).
212
213 **Disordered intestinal bacteria in IEC$^{\Delta Chil1}$ mice contribute to colitis.**
214
215 From the above data, it is evident that Chi3l1 is secreted into the intestinal mucus to influence the
216 colonization of Gram-positive bacteria, particularly *Lactobacillus*. We are now interested in
217 understanding the role of Chi3l1-regulated microbiota in a pathological condition. We observed a
218 significant increase in *Chil1* mRNA expression in the colon tissues of patients with either Crohn's
219 disease (CD) or Ulcerative colitis (UC) compared to normal tissues (Fig. 5A). To investigate
220 further, we created a colitis mouse model by subjecting Villin-cre and IECΔChil1 mice to a 2%

221 dextran sulfate sodium (DSS) diet for 7 days (Fig. 5B). The severity of colitis was assessed based
222 on weight loss, colon length, and tissue damage. Without the DSS challenge, the colon length and
223 structure were similar between Villin-cre and IEC$^{\Delta Chil1}$ mice (Fig. 5D&E). However, upon DSS
224 challenge, the IEC$^{\Delta Chil1}$ mice showed significantly shorter colon length, faster body weight loss,
225 and more severe inflammation compared to the Villin-cre mice (Fig. 5C-E).
226
227 To rule out the effects of Chi3l1 on the host contributed to colitis, we pretreated the mice with
228 antibiotics to eliminate gut microbiota before inducing colitis (Supplementary Figure 4A). The
229 Universal bacterial 16S rRNA qPCR data indicated that the majority of gut microbiota were
230 eliminated after antibiotics treatment (Supplementary Figure 4B). However, the IEC$^{\Delta Chil1}$ mice
231 exhibited a milder colitis phenotype, including slower body weight loss, longer colon length, and
232 less inflammation compared to the Villin-cre mice (Supplementary Figure 4C-E). We believe that
233 this could be due to the relationship between Chi3l1 and inflammation. Based on these findings, it
234 is apparent that Chi3l1's effects on gut microbiota play a more significant role in colitis.
235
236 To further elucidate the role of Chi3l1-regulated gut microbiota in colitis, we conducted fecal
237 microbiota transplantation (FMT) and *Lactobacillus reuteri* transplantation experiments. We first
238 eliminated gut microbiota through a 10-day course of antibiotics and then performed FMT from
239 Villin-cre mice or administered oral gavage of *Lactobacillus reuteri* to IEC$^{\Delta Chil1}$ mice for 2 weeks,
240 followed by a 7-day period of 2% DSS feeding (Fig 5F). FMT partially restored the colon length
241 of IEC$^{\Delta Chil1}$ mice to that of Villin-cre mice after the DSS challenge, but did not have an impact on
242 body weight loss or the level of inflammation in the gut (Fig. 5G-I). IEC$^{\Delta Chil1}$ mice transplanted
243 with *Lactobacillus* displayed a similar colitis phenotype as Villin-cre mice, characterized by
244 similar weight loss, colon length reduction, and gut inflammation (Fig. 5G-I). These findings
245 further validate the notion that Chi3l1-regulated gut microbiota, especially *Lactobacillus*, offers
246 protection against colitis.
247
248 **Discussion**
249
250 The intricate relationship between gut bacteria and their host organisms is crucial for health,
251 maintained through co-evolution and co-speciation. Understanding how the host influences these
252 bacterial communities is critical to understand the complex interplay between host and gut
253 bacteria. In this study, we discovered that Chi3l1 interacts with gut microbiota via peptidoglycan,
254 aiding the mucus colonization of beneficial bacteria like *Lactobacillus*, which protects against
255 colitis (Fig. 6). Our "scaffold model" demonstrates that Chi3l1 binds to bacterial peptidoglycan,
256 helping anchor and organize bacteria within the mucus layer. This interaction promotes the
257 colonization of beneficial bacteria, enhancing gut health.
258
259 Several studies have suggested a potential correlation between Chi3l1 and bacteria. For instance, it
260 has been demonstrated that Chi3l1 is produced by intestinal epithelial cells in enteritis disease and
261 aids in the elimination of pathogenic bacteria in the gut by neutrophils[24]. Another study
262 observed an increase in Chi3l1 expression in mammary tissues of dairy cows infected with
263 pathogenic *E. coli*, which promoted the recruitment of neutrophils[25]. Furthermore, Chi3l1 was
264 found to be induced during *Streptococcus pneumoniae* infection, where it enhanced bacterial

elimination by preventing the death of lung macrophages and improving host tolerance[26]. One study demonstrated that Chi3l1 contributes to the pathogenesis of colitis, possibly by facilitating the adhesion and invasion of bacteria onto colonic epithelial cells. However, we observed the presence of the Gram-negative bacterium *Salmonella typhimurium* in the mice used in their study[27]. According to standard for SPF-grade mice, Salmonella should not be present in laboratory mice, and it was also not detected by our 16S RNA sequencing. However, if mice are inadvertently infected with Salmonella in the context of IBD, it could likely exacerbate the development of IBD. Our data also demonstrate that Chi3l1 can bind to Gram-negative bacteria (Figure 2B). Therefore, the role of Chi3l1 on microbiota or IBD is heavily dependent on the environmental context. Another study found that caffeine treatment reduce Chi3l1 RNA expression levels, alleviate colitis, and decrease bacterial translocation[28]. However, previous research suggested that caffeine can directly inhibit inflammasome activation by suppressing MAPK/NF-κB signaling pathways[29]. Therefore, caffeine treatment may directly reduce colitis by inhibiting inflammation. Moreover, an additional control group of mice with Chi3l1 specifically knocked out in the gut is needed to examine the role of caffeine in the alleviation of colitis. However, the detailed mechanism of the interaction between Chi3l1 and the gut microbiota remains incompletely understood, partly due to the absence of Chi3l1-specific knockout mice and variations in mouse husbandry conditions. Here, by using intestinal Chi3l1-specific knockout mice, we demonstrated a new function of Chi3l1 in gut, which shapes bacterial colonozation through direct interaction with bacterial cell wall component, PGN. Moreover, Chi3l1-regulated gut microbiota, especially *Lactobacillus*, offers protection against colitis.

The bacterial cell wall is a complex structure mainly composed of peptidoglycan, but it may also contain other components such as teichoic acids and lipoteichoic acid in gram-positive bacteria, or an outer membrane containing various polysaccharides, lipids, and proteins in gram-negative bacteria[30]. Our findings indicated that lipopolysaccharide (LPS), a component of the bacterial cell wall, can slightly increase Chi3l1 expression (Fig. 1F&G), but higher levels of LPS do not further enhance Chi3l1 expression (data not shown). This suggests that there might be other components of the cell wall that can induce Chi3l1 expression in intestinal epithelial cells. Given the structural similarity between chitin and peptidoglycan (Fig. 2A), it is likely that Chi3l1 binds to the polysaccharide chains rather than the tetrapeptide in peptidoglycan. Previous studies have investigated the crystal structure of human Chi3l1 in complex with chitin, revealing a binding groove with different subsites for chitin fragments[31]. Other studies have also identified specific amino acids in chitinases that play a key role in the interaction with chitin[32, 33]. Nevertheless, further investigation is necessary to better understand the binding sites in Chi3l1 for peptidoglycan.

In the colon, there are two distinct parts of the mucus layer. The inner layer is attached and has a low number of microbes, while the outer layer is looser and densely populated by microorganisms. [34]. The diversity of bacteria in the mucus layer is similar to that found in the gut lumen[35]. It has to be noted that not all Gram-positive bacteria were reduced in Chil1$^{-/-}$ mice, as we found an increase in *Turicibacter* in the colon (Fig. 3G) and feces (data not shown). We believe this may be due to a combined effect of the host and gut microbiota. Another important factor for microbial growth in the colon is the integrity of the mucus barrier[11].We noticed a thinning of the mucus barrier in the mice lacking Chi3l1 compared to normal mice (Supplementary Figure 3 A&B).

However, we did not observe an increase in mucin-degrading bacteria such as *Bacteroides* or *Allobaculum*[36, 37] or a decrease in mucin-producing cells in these mice. We think that there may be bacteria that aid in the formation of the gut mucus, and these bacteria are decreased in mice lacking Chi3l1. Recent studies have introduced an "encapsulation model" regarding the nature of mucus in the colon. According to this model, the mucus in the proximal colon forms a primary encapsulation barrier around fecal material, while the mucus in the distal colon forms a secondary barrier.[38] Our findings indicate that Chi3l1 is expressed throughout the entire colon, including the proximal, middle, and distal sections (data not shown). This suggests that Chi3l1 likely promotes bacterial colonization across the entire colon. Despite most mucus being expelled with feces, the constant production of mucus and the minimal presence of Chi3l1 in feces (Figure 4C) indicate that Chi3l1 continuously plays a role in promoting the colonization of microbiota.

In patients with inflammatory bowel disease (IBD), the density and diversity of the microbial community in the intestines are reduced. Specifically, there is a decrease in *Firmicutes* and an increase in *Bacteroides* and facultative anaerobic bacteria like *Enterobacteriaceae*[39]. However, the cause of colitis in IBD is still a subject of debate. Our data suggest that disruptions in the gut microbiota contribute to colitis. In summary, our study demonstrates that bacterial challenge induces the expression of Chi3l1 in intestinal epithelial cells. Once produced, Chi3l1 is released into the mucus layer where it interacts with the gut microbiota, particularly through peptidoglycan, a primary component of bacterial cell walls. This interaction is beneficial for the colonization of bacteria, especially gram-positive bacteria like *Lactobacillus*, in the mucus layer. Dysbiosis resulting from a lack of Chi3l1 exacerbates DSS-induced colitis, highlighting the role of dysbiosis as a contributing factor to colitis.

Methods

Animal experiments and procedures.

C57BL/6J (Strain No. N000013), Germ-free (Strain No. N000295), Chil1$^{fl/fl}$ (Strain No. T013652), Chil1$^{-/-}$ (Strain No. T014402) mice were purchased from GemPharmatech. Villin-cre mice were provided by Dr. Qun Lu (Yunnan University, China,). All mouse colonies were maintained at the animal core facility of Yunnan University. C57BL/6J was used as wildtype control since Chil1$^{-/-}$ mice are on the C57BL/6J background, as determined by PCR (data not shown). The animal studies described have been approved by the Yunnan University Institutional Animal Care and Use Committee (IACUC, Approval No. YNU20220256). Female mice aged 8-10 weeks old were used in most studies.

Genotyping Tail clippings were placed in 1.5 ml tubes with 75 µL of master mix solution (60 µL H_2O, 7.5 µL 250 mM NaOH, 7.5 µL 2 mM EDTA) and incubated at 98°C for 1 hour. After cooling to 15°C, 75 µL of neutralization buffer (40 mM Tris HCl, pH 5.5) was added, and the samples were centrifuged at 4000 rpm for 3 minutes. A 1:10 dilution was prepared by mixing 2 µL of supernatant with 18 µL of water for genotyping PCR. A 25 µL PCR reaction mix was prepared with 12.5 µL of 2x Taq Master Mix (Dye Plus, Vazyme P112-03), 1 µL of each primer, 2 µL of template, and water. PCR was conducted using a Biorad machine with the following program:

353 95°C for 5 minutes; 98°C for 30 seconds; 65°C with a 0.5°C decrement per cycle for 30 seconds;
354 72°C for 45 seconds, repeating steps 2-4 for 20 cycles; 98°C for 30 seconds; 55°C for 30 seconds;
355 72°C for 45 seconds, repeating steps 5-7 for 20 cycles; 72°C for 5 minutes; and hold at 10°C.
356 Primer sequences are listed in Table S1.
357
358 **Table S1**

Aim genes	PCR No.	Primer No.	Sequence	Band Size
flox	① 5'arm (flox)	F1(JS05000-Chil1-5wt-tF1)	CTTGTTCAGCCAAG GTGATGGGTA	WT:270bp targeted:375bp
		R1(JS05000-Chil1-5wt-tR1)	CTACCTGATTGCTG GGGCTCATTA	
	② 3'arm	F2(JS15000-Chil1-3wt-F1)	CCAGTATTTAGAGG CAGAGAGATGGTG	WT:283bp targeted:384bp
		R2(JS15000-Chil1-3wt-R1)	CTCGAATTCAGAAA TCTGCCTGCCT	
Chil1$^{-/-}$	①	F1(JS05000-Chil1-5wt-tF1)	CTTGTTCAGCCAAG GTGATGGGTA	WT: 2960 bp Targeted: ~256 bp
		R1(JS05000-Chil1-3wt-tR1)	CTCGAATTCAGAAA TCTGCCTGCCT	
	②	F2(JS15000-Chil1-wt-F1)	CTGTTAGTTGCACC TTGGAGCAGTCA	WT: 309 bp Targeted:0 bp
		R2(JS15000-Chil1-wt-R1)	CAGATATAGGAGA ACATCCAGTCTGGG	
Chil1-reporter	①	EGE-YQH-063-A-WT-F	CAGTTTCCCAACCC CTCACCTC	Targeted:485 ~bp
		EGE-YQH-063-A-Mut-R	AAGAAGTCGTGCTG CTTCATGTGGT	
	②	EGE-YQH-063-A-WT-F	CAGTTTCCCAACCC CTCACCTC	WT:323 Targeted:1106~ bp
		EGE-YQH-063-A-WT-R	CTACCCTAGTTCCCT GTTCTCCA	
Cre	Cre①	Cre1	AGGTTCGTTCACTC ATGGA	Cre:250bp Internal Control (Fabpi)=480bp
		Cre2	TTCGACCAGTTTAG TTACCC	
	IntC500②	IntC500F	CCTCCGGAGAGCAG CGATTAAAAGTGTC AG	
		IntC500R	TAGAGCTTTGCCAC ATCACAGGTCATTC AG	

359
360 *Rectal administration of FDAA-labeled E. faecalis* For FDAA-labeled *E. faecalis*, *E. faecalis*
361 were grown in LB media until reaching mid-exponential phase, approximately 4 hours. FDAA
362 was then added to the culture media to a final concentration of about 17 μM. The *E. faecalis*
363 continued to grow for 4 hours and were then harvested by centrifugation (5000 x g for 10 min),
364 washed, and resuspended in PBS at a density of $5x10^9$ CFU/ml. For rectal administration,
365 wildtype and Chil1$^{-/-}$ mice were fasted overnight (5:00pm to 9:00am) before intraperitoneally (i.p.)

366 injecting them with 400mg/kg tribromoethanol (Nanjing AIBI BioTechnology, M2910), followed
367 by rectal injection of $1x10^9$ FDAA-labeled E. faecalis in 200 μl PBS via a flexible catheter. The
368 catheter was inserted into the anus to a depth of 4.5 cm, and the *E. faecalis* were injected slowly to
369 avoid overflow. The mice were then kept upside down for approximately 2 minutes. After 4 hours
370 of rectal injection, the mice's colons were collected and immediately embedded in OTC
371 embedding medium for observation on 5μm thick frozen sections. OP50-mCherry ($1x10^9$
372 CFU/mice) treated same as *E. faecalis*.
373
374 *DSS-induced mouse colitis* Villin-cre and $IEC^{\Delta Chil1}$ mice were fed a 2% dextran sodium sulfate
375 (DSS, MP, 9011-18-1) solution in their drinking water for 7 days. The mice's body weight was
376 monitored daily during the feeding period. After the 7-day DSS treatment, the mice were
377 sacrificed. Colons were collected, and their length was measured from the cecum to the rectum.
378 Colon paraffin sections were harvested, and H&E staining was performed to examine gut
379 inflammation.
380
381 *Antibiotics treatment* $IEC^{\Delta Chil1}$ mice were fed an antibiotics mixture containing 0.5 mg/ml of
382 Metronidazole (Solarbio, M8060), 1 mg/ml of vancomycin (Solarbio, V8050), 1 mg/ml of
383 Ampicillin (Solarbio, A8180), and 0.5 mg/ml of Neomycin Sulfate (Solarbio, N8090) in their
384 drinking water for 7 days (approximately 5ml per mouse per day). After the 7-day antibiotics
385 treatment, the mice were orally gavaged with 200μl of the antibiotics mixture for another 3 days.
386 Microbiota depletion was examined in feces using 16S rRNA qPCR on the 10th day of antibiotics
387 feeding.
388
389 *Fecal microbiota transplantation (FMT)* Fresh feces were collected from 8-10 weeks old Villin-
390 cre mice and immediately snap-frozen in liquid nitrogen. On the experimental day, feces were
391 resuspended in PBS to a concentration of 200 mg/ml and centrifuged at 350g for 5 minutes to
392 collect the supernatant. Antibiotics pre-treated $IEC^{\Delta Chil1}$ mice were orally gavaged with 10 μl of the
393 dissolved feces per gram of mouse weight for 14 days.
394
395 *Oral gavage of Lactobacillus reuteri* *Lactobacillus reuteri* was grown in MRS broth at 37°C for
396 48 hours under anaerobic conditions. The bacteria were harvested by centrifugation (5000 x g for
397 10 min), washed, and resuspended in PBS at a density of OD_{605}=1.2-1.3/ml. Antibiotics pre-
398 treated $IEC^{\Delta Chil1\ mice}$ were orally gavaged with 200μl of the dissolved Lactobacillus reuteri per
399 mouse for 14 days.
400
401 **Bacterial colony identification**
402 Fresh feces were collected from 8-week-old wild-type mice and dissolved in LB culture medium.
403 The dissolved feces were then cultured at 37°C for 12 hours and plated onto LB agar plates. The
404 grown colonies were picked using sterile pipette tips and resuspended in 20 μl of sterile water. A
405 PCR reaction was performed using 2 μl of the bacterial suspension as template DNA and universal
406 bacterial 16S rRNA primers (27F, 5'-AGAGTTTGATCCTGGCTCAG-3' and 1492R, 5'-
407 GGTTACCTTGTTACGACTT-3') with reaction conditions: 95°C for 5 min followed by 35 cycles
408 of 95°C for 30sec, 55°C for 30sec, 72°C for 2min and then 72°C for 20min. The amplicons were
409 then sequenced, and the resulting sequences were analyzed using BLASTN and the NCBI

410 database for species identification.
411
412 **Treatment of DLD-1 cells with live, heat-killed bacteria or LPS**
413 Bacteria harvested from mouse feces or specific strains were grown in LB medium at 37°C for 12
414 hours under aerobic conditions. The bacteria were then collected by centrifugation (5000 x g for
415 10 min), washed, and resuspended in PBS at a density of 1.2 x 10^{10} CFU/ml. Live bacteria were
416 used directly, while heat-killed bacteria required further heating at 80°C for 30 minutes. DLD-1
417 cells were grown in DMEM medium supplemented with 10% FBS. Prior to treatment, the cells
418 were replated and allowed to reach 80% confluency. Either live or heat-killed bacteria were added
419 to the cells at a multiplicity of infection of 20 each well, and 100 pg/ml LPS treatment(Sigma,
420 L4392; diluted in PBS) was also performed. After 12-hour incubation, cellular proteins were
421 extracted for western blot analysis or the cells were subjected to immunofluorescent staining.
422
423 **Cell Culture and Bacterial Adhesion Assay**
424 DLD-1 cells were cultured in 6-well plates until they reached approximately 80% confluency per
425 well. The cells were then washed three times with PBS to remove any residual antibiotics. Fresh
426 DMEM supplemented with 10% FBS (without antibiotics) was added to the cells. E. coli strains
427 were introduced to each well at a multiplicity of infection (MOI) of 20 and incubated for 2.5 hours
428 at 37°C. After incubation, the cells were washed three times with PBS. For the adhesion assays,
429 the cells were lysed with 1 mL of 1% Triton-X100 (BBI, 9002-93-1) in deionized water for 30
430 minutes. The cell lysates were then plated onto Luria broth (LB) agar plates at various dilutions
431 and incubated overnight at 37°C. The following day, colonies were counted and calculated as
432 colony-forming units (CFU)/mL.
433
434 **shRNA Lentivirus Packaging and Transfection**
435 For the packaging of shRNA lentivirus, shRNA control and Chi3l1 shRNA1 lentiviruses were
436 packaged in 293T cells. The cell culture medium containing the virus was collected and stored at -
437 80°C. For transfection of DLD-1 cells, the cells were cultured in 6-well plates until they reached
438 approximately 80% confluency. The cell culture medium was then replaced with a mixture of
439 culture medium containing the virus and fresh cell culture medium in a 1:1 ratio. Following
440 transfection, the bacterial adhesion assay was performed as described above.
441
442 **Bacterial or peptidoglycan binding assay**
443 Different bacteria strains were grown in LB medium at 37°C for 12 hours under aerobic
444 conditions. The bacteria were collected by centrifugation (5000 x g for 10 min), washed, and
445 resuspended in MES buffer (25mM MES, 25mM NaCl, Ph=6.0) at a density of 5x10^9 CFU/ml.
446 1μg Recombinant mouse Chi3l1 (rmChi3l1) was added to the bacterial suspension and incubated
447 at 4°C under rotation overnight. Supernatant, wash fractions, and bacterial-bound fractions were
448 collected and analyzed using western blot analysis. For the peptidoglycan binding assay, 1μg
449 rmChi3l1 or recombinant human Chi3l1 (rhChi3l1) and bovine serum albumin (BSA) was
450 incubated with 100μg peptidoglycan (PGN). The incubation and wash procedure were similar to
451 the bacterial binding assay, and the proteins in each fraction were analyzed using silver staining or
452 western blot.
453

Hematoxylin/eosin(H&E) and Periodic acid-Schiff and Alcian blue (AB-PAS) staining

Tissues were fixed with buffered 10% paraformaldehyde (BI, E672001-0500) overnight at 4°C and embedded in paraffin. Ultra-thin tissue slices (5μm) were prepared and deparaffinized. H&E staining was performed on the tissue sections, and slides were examined under a microscope (Leica). For AB-PAS staining, tissues were fixed in Carnoy's solution (60% Ethanol， 30% Chloroform， 10% Acetic Acid) for 24 hour at 4°C and embedded in paraffin. AB-PAS staining (Solarbio, G1285) was performed according to the manufacturer's protocol. The staining was visualized under the microscope (Leica).

Immunohistochemical (IHC) and immunofluorescent (IF) staining

Tissue paraffin sections were prepared as previously described for H&E staining. Antigen retrieval was performed by treating the sections with citric acid (pH 6.0) at 95°C for 15 minutes, followed by cooling to room temperature. The sections were then washed with PBS and ddH2O. To block any nonspecific binding, a blocking buffer containing 5% goat serum, 3% BSA, and 0.1% Triton X-100 in PBS was applied to the sections for 1 hour at room temperature in a humidity chamber. The sections were then incubated with anti-Chi3l1 primary antibodies (Invitrogen, PA5-95897, 1:200), followed by staining with Goat anti-Rabbit IgG (H+L) Secondary Antibody-Biotin (Invitrogen, 65-614, 1:2000). Finally, the sections were stained with Horseradish Peroxidase conjugate antibody (Invitrogen, A2664, 1:2000) and developed with DAB for 10 minutes. The slides were examined under a microscope (Leica).

Immunofluorescent staining was also performed on paraffin sections using specific primary antibodies. These included anti-MUC2 (Invitrogen, PA5-103083, 1:50), anti-Chi3l1 (Abcam, ab180569, 1:400; antigen retrieval with Tris-EDTA at pH 9.0), anti-ChgA (Santa Cruz, sc-393941, 1:200; antigen retrieval with citrate at pH 6.0), anti-UEA-1-FITC (GeneTeX, GTX0151, 1:200; antigen retrieval with citrate at pH 6.0), and anti-LTA (Invitrogen, MA1-7402, 1:50). The secondary antibodies used were 488-conjugated Affinipure Goat Anti-Rabbit IgG(H+L) (Jackson ImmunoResearch, 111-545-003, 1:1000) and 594-conjugated Goat Anti-Mouse IgG (H+L) (Jackson ImmunoResearch, 115-585-003, 1:1000). Slides were washed and mounted with antifade medium (Vectashield, H-1000-10). Nuclei were stained with DAPI (Beyotime, c1006, prediluted). Images were captured using a fluorescence microscope (Leica, 2084 DP-80).

Immunofluorescent staining on DLD-1 cells, cells were seeded on coverslips in 12-well plate and challenged with 100 pg/ml LPS (Sigma, L4391; diluted in PBS) for 12 hours. Cells were washed with cold-PBS twice gently, then fixed with 2% paraformaldehyde in PBS at room temperature for 10 min. After removal of fixation buffer and wash twice with cold-PBS, cells were blocked with blocking buffer (3% BSA, 0.5% Triton-X-100 in PBS) for 1 hour in humidity chamber at room temperature. Rabbit anti-Chi3l1 antibody (Proteintech, 12036-1-AP; 1:200) was applied at room temperature for 1 hour. After wash with 1 x TBST three times, secondary antibody AlexaFluor 488 (Jackson ImmunoResearch, 111-545-003, 1:1000) was applied for another 1 hour at room temperature in a humidified chamber under darkness. Finally, cells were counterstained with DAPI (beyotime, C1006) and mounted onto slides. Images were captured using an Olympus BX53F2 microscope.

498 **Fluorescence in situ hybridization (FISH)**
499 Murine intestinal paraffin sections were prepared according to the previously described method
500 for H&E staining. The tissues sections were rehydrated using a graded ethanol series and then
501 washed with distilled water. The gram-positive bacterial probe, consisting of three different
502 sequences (/5Alex550N/TGGAAGATTCCCTACTGC/3AlexF550N/,
503 /5Alex550N/CGGAAGATTCCCTACTGC/3AlexF550N/,
504 /5Alex550N/CCGAAGATTCCCTACTGC/3AlexF550N/), or the control nonspecific probe
505 (/5Alex550N/ACTCCTACGGGAGGCAGC/3AlexF550N/), was diluted to a concentration of 100
506 nM in FISH hybridization buffer (containing 20 mM Tris pH 7.2, 0.9 M NaCl, and 0.1% SDS) and
507 applied to the slides. The slides were then incubated overnight at 56°C in a humidified chamber.
508 Following incubation, the slides were washed and the nuclei were counterstained with DAPI. The
509 images were captured using a fluorescence microscope (Leica, 2084 DP-80).
510
511 **Immunoblot and silver staining**
512 Protein extraction from cultured cells involved lysing the cells in 2% SDS lysis buffer, which is
513 prepared by dissolving 2g of SDS powder in 100ml of sterilized ddH2O. Bacteria or
514 peptidoglycan precipitates were resuspended in MES buffer, which contained 25mM MES, 25mM
515 NaCl, and had a pH of 6.0. For protein extraction from mice ileum and colon tissues, 30mg of
516 snap-frozen tissues were homogenized in 1ml of RIPA buffer, which contained 10mM Tris-HCl
517 (pH 8.0), 1mM EDTA, 0.5mM EGTA, 1% TritonX-100, 0.1% sodium deoxycholate, 0.1% SDS,
518 140mM NaCl, 1mM PMSF, and a proteinase inhibitor. The lysates were then supplemented with
519 5x SDS loading buffer to a final concentration of 1x. The resulting mixture was subsequently
520 boiled at 100°C for 10 minutes and centrifuged at 4°C and 12,000 rpm for 10 minutes. The
521 supernatants were collected for western blot analysis. The supernatants were separated using a
522 10% SDS-PAGE gel and then transferred to a polyvinylidene fluoride membrane. The membranes
523 were blocked with 5% nonfat milk in TBST buffer (containing 0.1% Tween-20 in tris-buffered
524 saline) and sequentially incubated with primary antibodies and appropriate horseradish peroxidase
525 (HRP)-conjugated secondary antibodies. Protein bands were detected using enhanced
526 chemiluminescence (ECL) reagent with a Minichemi Chemiluminescence Imaging System. The
527 primary antibodies used included anti-Chi3l1 (RD, MAB2649, 1:2000) and anti-alpha-Actinin
528 (Cell Signaling, 69758S, 1:1000). The secondary antibodies used were goat anti-Rat-IgG (Cell
529 Signaling, 7077s, 1:1000) and goat anti-mouse (Invitrogen, 62-6520, 1:1000). For silver staining,
530 the PAGE gel was subjected to silver staining using a fast-silver staining kit (Beyotime, P0017S)
531 following the manufacturer's instructions.
532
533 **DNA extraction for 16S rRNA analysis**
534 For isolation of luminal contents from murine ileum and colon, a 9 cm section of ileum and 3 cm
535 section of colon were cut open longitudinally, and luminal contents were scratched off into a pre-
536 weighed 2-ml sterile freezing vial. The weight of the contents was recorded for further processing.
537 For isolation of mucus from murine ileum and colon, tissues were flushed with 2 ml of ice-cold
538 PBS into a pre-weighed 2-ml sterile freezing vial after removal of the liminal contents. The mucus
539 was then pelleted by centrifugation at 10,000g for 10 minutes, and the supernatant was removed.
540 For feces isolation, fresh murine feces were collected into a sterile freezing vial weighing 2 ml,
541 and immediately snap-frozen in liquid nitrogen. For bacterial DNA extraction, DNA was extracted

542 and purified following the manufacture's protocol using the EIANamp stool DNA kit (TIANGEN,
543 DP328-02).
544
545 **Microbiota 16S rRNA gene sequencing**
546 Fecal samples, ileum contents, and colon contents were collected from wildtype, Chil1$^{-/-}$
547 littermates, or Villin-cre, IEC$^{\Delta Chil1}$ littermates and immediately frozen in liquid nitrogen. The
548 microbial genomic DNA was extracted and 16S rRNA sequencing was performed by Biomarker
549 Technologies. The hypervariable regions V3 and V4 of the bacterial 16S rRNA gene were
550 sequenced using universal primers that flank these regions V3 (338F 5'-
551 ACTCCTACGGGAGGCAGCA-3') and V4 (806R 5'- GGACTACHVGGGTWTCTAAT-3'). The
552 sequencing was done using the IIIumina Sequencing platform. The resulting 16S rRNA gene
553 sequences were analyzed using scripts from the BMK Cloud platform (www.biocloud.net). The
554 microbial classification was performed using the SILVA138 and hierarchical clustering algorithms.
555 The OTUs were determined by clustering the sequences with 97% similarity and were classified
556 into different taxonomic ranks. The relative abundance of each bacterial species was visualized
557 using R software. The raw 16S rRNA gene sequencing data can be accessed on the BMKCloud
558 platform under the project ID Microbial_updateReport_20211221092022313.
559
560 **16S qPCR analysis**
561 Quantitative PCR was performed using SYBR green master mix (Thermo Fisher, A25742) in
562 triplicates. This was done on a Real-Time PCR QuatStudio1 with accompanying software,
563 following the instructions provided by the manufacturer (Life Technologies, Grand Island, NY,
564 USA). The abundance of specific bacterial groups in the intestine was determined using qPCR
565 with either universal or bacteria-specific 16S rRNA gene primers. Standard curves were
566 constructed with *E.Coli OP50* 16S rRNA gene, which was amplified using conserved 16S rRNA
567 primers. It should be noted that qPCR measures the number of 16S gene copies per sample, not
568 the actual bacterial numbers or colony forming units. Primer sequences are provided in table S2.
569
570 **Table S2**
571 **qPCR primers**

Targeted bacteria	Primer No.	Sequence
Universal	27F	AGAGTTTGATCCTGGCTCAG
	1492R	GGTTACCTTGTTACGACTT
Gram-positive	928F–firm	TGAAACTYAAGGAATTGACG
	1040-firmR	ACCATGCACCACCTGTC
Lactobacillus	F	TGGAAACAGGTGCTAATACCG
	R	GTCCATTGTGGAAGATTCCC

572
573 **Key source tables**
574
575 **Antibodies and chemicals**

Reagent or Antibodies	Source	Indentifier
Dextran Sulfate Sodium Salt	MP	CAS:9011-18-1
AB-PAS staining kit	Solarbio	G1285
EIANamp stool DNA kit	TIANGEN	DP328-02
PAGE Gel Fast Preparation Kit	Shanghai Epizyme biotechnology	PG113

gel extraction kit	Omega--	D2500-02
SYBR Green kit	Thermo Fisher	A25742
hematoxylin	Servicebio	G1004
eosin	Biosharp	BL703b
DAB Substrate Kit	ZSGB-BIO	zli-9018
Tris	Solarbio	77-86-1
Sodium chloride	Solarbio	7647-14-5
disodium salt dihydrate (EDTA)	Sangon Biotech	6381-92-6
Sodium dodecyl sulfate (SDS)	BBI	A601336-0500
egtazic acid,Glycol ether diamine tetraacetic acid (EGTA)	BBI	67-42-5
TritonX-100	BBI	9002-93-1
Citric acid	Sangon Biotech	77-92-9
Vancomycin	Solarbio	V8050
Ampicillin- Sodium salt	Solarbio	A8180)
Metronidazole	Solarbio	M8060
Neomyein Sulfate	Solarbio	N8090
MRS broth	Solarbio	M8540
Goat serum	Solarbio	
Anti-Chi3l1 Polyclonal Antibody	Invitrogen	PA5-95897
Cha-A antibody	Santa Cruz	sc-393941
anti-mouse Chi3l1 Purified Rat Monoclonal IgG	R&D	MAB2649
MUC2 Polyclonal Antibody	Invitrogen	PA5-103083
Gram Positive Bacteria LTA Monoclonal Antibody (G43J)	Invitrogen	MA1-7402
488-conjugated Affinipure Goat Anti-Rabbit	Jackson	111-545-003
immunoresearch Alexa Fluor 594 AffiniPure Goat Anti-Mouse IgG (H+L)	Jackson	115-585-003
Goat anti-Rabbit IgG (H+L) Secondary Antibody-Biotin	Invitrogen	65-6140
Horseradish Peroxidase conjugate antibody	Invitrogen	A2664
Rabbit anti-Chi3l1 antibody	Proteintech	12036-1-AP
Goat anti-Rabbit IgG	Jackson ImmunoResearch	111-035-0030
Mouse anti-α-tubulin antibody	sigma	T5168
Goat anti-mouse IgG	Jackson ImmunoResearch	115-035-003
Goat anti-Rat IgG	Jackson ImmunoResearch	112-035-003
DAPI	Beyotime	c1006
Antifade mounting medium	Vectashield	H-1000-10
FDAA	5TAMRA; CHINESE PEPTIDE	CS-11-00433
gram-positive bacteria 16S rRNA probe	Guangzhou Exon Biotech	

576

577 **Cell lines/ Bacteria strains**

DLD-1 cells	a gift from Dr. Sun Jianwei at Yunnan University	
Staphylococcus saprophyticus	ATCC	15305
E. faecalis	ATCC	33186
Lactobacillus reuteri	ATCC	23272
E. coli strain *K12*	Dharmacon	Cat #OEC5042

E. coli strain OP50	CGC	RRID:WB STRAIN:OP50
E. coli strain OP50-mCherry	Provided by Bin Qi Lab	[40]
Staphylococcus Sciuri	identified from C57BL/6J wild-type mice stools	
E. coli	identified from C57BL/6J wild-type mice stools	

Statistical analysis

Data were presented as mean ± SEM. Statistical analyses were carried out using GraphPad Prism (GraphPad Software). Comparisons between two groups were carried out using unpaired Student t test. Comparisons among multiple groups (n>=3) were carried out using one-way ANOVA. P values are as labeled and less than 0.05 was considered not significant. Patient data were analyzed by Mann-Whitney test.

Author Contributions

Y.C. and R.Z.Y. performed experiments, analyzed data, and wrote the manuscript. B.Q. organized and designed the study. Z.S. initiated, organized, designed the study and wrote the manuscript.

Acknowledgements

We thank Qun Lu (Yunnan University) for providing Villin-cre mice. We thank Wenxiang Fu (Yunnan University) for imaging technical support. We thank Jianwei Sun (Yunnan University) for providing DLD-1 cell line. We thank Zehan Hu (Shanghai Jiao Tong University) for methods of bacteria 16S FISH staining. This work was supported by Ministry of Science and Technology of China (2019YFA0803100, 2019YFA0802100 to B.Q.), National Natural Science Foundation of China (32071129 to Z.S., 32170794 to B.Q.), Yunnan Fundamental Research Projects (202101AT070022, 202001AW070006 to Z.S., 202201AT070196 to B.Q.), Science and Technological Talent Cultivation Plan of Yunnan Province (C619300A086 to Z.S., K264202230211 to B.Q.), Yunnan Provincial Science and Technology Project at Southwest United Graduate School (202302AP370005 to B.Q.)

Declaration of interests

The authors declare no competing interests.

Reference

[1] C. A. Lozupone, J. I. Stombaugh, J. I. Gordon, J. K. Jansson, and R. Knight, "Diversity, stability and resilience of the human gut microbiota," (in English), *Nature,* vol. 489, no. 7415, pp. 220-230, Sep 13 2012.

[2] M. R. Charbonneau *et al.*, "A microbial perspective of human developmental biology," *Nature,* vol. 535, no. 7610, pp. 48-55, Jul 7 2016.

[3] J. L. Sonnenburg and F. Backhed, "Diet-microbiota interactions as moderators of human

metabolism," (in English), *Nature,* vol. 535, no. 7610, pp. 56-64, Jul 7 2016.

[4] C. A. Thaiss, N. Zmora, M. Levy, and E. Elinav, "The microbiome and innate immunity," *Nature,* vol. 535, no. 7610, pp. 65-74, Jul 7 2016.

[5] K. Honda and D. R. Littman, "The microbiota in adaptive immune homeostasis and disease," *Nature,* vol. 535, no. 7610, pp. 75-84, Jul 7 2016.

[6] A. J. Baumler and V. Sperandio, "Interactions between the microbiota and pathogenic bacteria in the gut," (in English), *Nature,* vol. 535, no. 7610, pp. 85-93, Jul 7 2016.

[7] C. Petersen and J. L. Round, "Defining dysbiosis and its influence on host immunity and disease," (in English), *Cellular Microbiology,* vol. 16, no. 7, pp. 1024-1033, Jul 2014.

[8] J. E. McDonald, J. R. Marchesi, and B. Koskella, "Application of ecological and evolutionary theory to microbiome community dynamics across systems," (in English), *Proceedings of the Royal Society B-Biological Sciences,* vol. 287, no. 1941, Dec 23 2020.

[9] J. I. Gordon, "Honor Thy Gut Symbionts Redux," (in English), *Science,* vol. 336, no. 6086, pp. 1251-1253, Jun 8 2012.

[10] J. X. Fu *et al.*, "Loss of intestinal core 1-derived O-glycans causes spontaneous colitis in mice," (in English), *Journal of Clinical Investigation,* vol. 121, no. 4, pp. 1657-1666, Apr 2011.

[11] M. E. V. Johansson, M. Phillipson, J. Petersson, A. Velcich, L. Holm, and G. C. Hansson, "The inner of the two Muc2 mucin-dependent mucus layers in colon is devoid of bacteria," (in English), *Proceedings of the National Academy of Sciences of the United States of America,* vol. 105, no. 39, pp. 15064-15069, Sep 30 2008.

[12] A. Swidsinski, J. Weber, V. Loening-Baucke, L. P. Hale, and H. Lochs, "Spatial organization and composition of the mucosal flora in patients with inflammatory bowel disease," (in English), *Journal of Clinical Microbiology,* vol. 43, no. 7, pp. 3380-3389, Jul 2005.

[13] M. E. V. Johansson *et al.*, "Bacteria penetrate the normally impenetrable inner colon mucus layer in both murine colitis models and patients with ulcerative colitis," (in English), *Gut,* vol. 63, no. 2, pp. 281-291, Feb 2014.

[14] D. Gevers *et al.*, "The Treatment-Naive Microbiome in New-Onset Crohn's Disease," (in English), *Cell Host & Microbe,* vol. 15, no. 3, pp. 382-392, Mar 12 2014.

[15] G. P. Donaldson *et al.*, "Gut microbiota utilize immunoglobulin A for mucosal colonization," *Science,* vol. 360, no. 6390, pp. 795-800, May 18 2018.

[16] C. G. Lee *et al.*, "Role of chitin and chitinase/chitinase-like proteins in inflammation, tissue remodeling, and injury," *Annu Rev Physiol,* vol. 73, pp. 479-501, 2011.

[17] D. R. Houston, A. D. Recklies, J. C. Krupa, and D. M. F. van Aalten, "Structure and ligand-induced conformational change of the 39-kDa glycoprotein from human articular chondrocytes," (in English), *Journal of Biological Chemistry,* vol. 278, no. 32, pp. 30206-30212, Aug 8 2003.

[18] M. Fulde *et al.*, "Neonatal selection by Toll-like receptor 5 influences long-term gut microbiota composition," (in English), *Nature,* vol. 560, no. 7719, pp. 489-+, Aug 23 2018.

[19] S. Vaishnava *et al.*, "The antibacterial lectin RegIIIgamma promotes the spatial segregation of microbiota and host in the intestine," *Science,* vol. 334, no. 6053, pp. 255-8, Oct 14 2011.

661 [20] M. Groussin, F. Mazel, and E. J. Alm, "Co-evolution and Co-speciation of Host-Gut
662 Bacteria Systems," *Cell Host Microbe,* vol. 28, no. 1, pp. 12-22, Jul 8 2020.
663 [21] D. R. Hill *et al.*, "Bacterial Colonization Stimulates a Complex Physiological Response in
664 the Immature Human Intestinal Epithelium," (in English), *In Vitro Cellular &*
665 *Developmental Biology-Animal,* vol. 54, pp. S6-S6, Jun 2018.
666 [22] T. Zhao, Z. Su, Y. Li, X. Zhang, and Q. You, "Chitinase-3 like-protein-1 function and its
667 role in diseases," *Signal Transduct Target Ther,* vol. 5, no. 1, p. 201, Sep 14 2020.
668 [23] W. Wang *et al.*, "Assessing the viability of transplanted gut microbiota by sequential
669 tagging with D-amino acid-based metabolic probes," *Nat Commun,* vol. 10, no. 1, p.
670 1317, Mar 21 2019.
671 [24] C. Deutschmann *et al.*, "Identification of Chitinase-3-Like Protein 1 as a Novel
672 Neutrophil Antigenic Target in Crohn's Disease," (in English), *Journal of Crohns & Colitis,*
673 vol. 13, no. 7, pp. 894-904, Jul 2019.
674 [25] K. Breyne *et al.*, "Immunomodulation of Host Chitinase 3-Like 1 During a Mammary
675 Pathogenic Escherichia coli Infection," (in English), *Frontiers in Immunology,* vol. 9, May
676 28 2018.
677 [26] C. S. Dela Cruz *et al.*, "Chitinase 3-like-1 promotes Streptococcus pneumoniae killing
678 and augments host tolerance to lung antibacterial responses," *Cell Host Microbe,* vol. 12,
679 no. 1, pp. 34-46, Jul 19 2012.
680 [27] E. Mizoguchi, "Chitinase 3-like-1 exacerbates intestinal inflammation by enhancing
681 bacterial adhesion and invasion in colonic epithelial cells," *Gastroenterology,* vol. 130, no.
682 2, pp. 398-411, Feb 2006.
683 [28] I. A. Lee, D. Low, A. Kamba, V. Llado, and E. Mizoguchi, "Oral caffeine administration
684 ameliorates acute colitis by suppressing chitinase 3-like 1 expression in intestinal
685 epithelial cells," (in English), *Journal of Gastroenterology,* vol. 49, no. 8, pp. 1206-1216,
686 Aug 2014.
687 [29] E. E. Vargas-Pozada *et al.*, "Caffeine Inhibits NLRP3 Inflammasome Activation by
688 Downregulating TLR4/MAPK/NF-κB Signaling Pathway in an Experimental NASH
689 Model," (in English), *International Journal of Molecular Sciences,* vol. 23, no. 17, Sep
690 2022.
691 [30] J. X. Zhou *et al.*, "Breaking down the cell wall: Still an attractive antibacterial strategy," (in
692 English), *Frontiers in Microbiology,* vol. 13, Sep 23 2022.
693 [31] F. Fusetti, T. Pijning, K. H. Kalk, E. Bos, and B. W. Dijkstra, "Crystal structure and
694 carbohydrate-binding properties of the human cartilage glycoprotein-39," (in English),
695 *Journal of Biological Chemistry,* vol. 278, no. 39, pp. 37753-37760, Sep 26 2003.
696 [32] S. Ferrandon, T. Sterzenbach, F. B. Mersha, and M. Q. Xu, "A single surface tryptophan in
697 the chitin-binding domain from Bacillus circulans chitinase A1 plays a pivotal role in
698 binding chitin and can be modified to create an elutable affinity tag," (in English),
699 *Biochimica Et Biophysica Acta-General Subjects,* vol. 1621, no. 1, pp. 31-40, Apr 7 2003.
700 [33] A. Ranok, J. Wongsantichon, R. C. Robinson, and W. Suginta, "Structural and
701 Thermodynamic Insights into Chitooligosaccharide Binding to Human Cartilage
702 Chitinase 3-like Protein 2 (CHI3L2 or YKL-39)," (in English), *Journal of Biological*
703 *Chemistry,* vol. 290, no. 5, pp. 2617-2629, Jan 30 2015.
704 [34] M. E. V. Johansson, J. M. H. Larsson, and G. C. Hansson, "The two mucus layers of colon

are organized by the MUC2 mucin, whereas the outer layer is a legislator of host-microbial interactions," (in English), *Proceedings of the National Academy of Sciences of the United States of America,* vol. 108, pp. 4659-4665, Mar 15 2011.

[35] Z. H. Hu *et al.*, "Small proline-rich protein 2A is a gut bactericidal protein deployed during helminth infection," (in English), *Science,* vol. 374, no. 6568, Nov 5 2021.

[36] S. Raimondi, E. Musmeci, F. Candeliere, A. Amaretti, and M. Rossi, "Identification of mucin degraders of the human gut microbiota," (in English), *Scientific Reports,* vol. 11, no. 1, May 27 2021.

[37] J. S. Glover, T. D. Ticer, and M. A. Engevik, "Characterizing the mucin-degrading capacity of the human gut microbiota," (in English), *Scientific Reports,* vol. 12, no. 1, May 19 2022.

[38] K. Bergstrom *et al.*, "Proximal colon-derived O-glycosylated mucus encapsulates and modulates the microbiota," (in English), *Science,* vol. 370, no. 6515, pp. 467-472, Oct 23 2020.

[39] J. J. Qin *et al.*, "A human gut microbial gene catalogue established by metagenomic sequencing," (in English), *Nature,* vol. 464, no. 7285, pp. 59-U70, Mar 4 2010.

[40] Y. J. He *et al.*, "N-glycosylated intestinal protein BCF-1 shapes microbial colonization by binding bacteria via its fimbrial protein," (in English), *Cell Reports,* vol. 42, no. 1, Jan 31 2023.

Main Figure legends

Figure 1. Intestinal epithelial cells express Chi3l1 induced by gut microbiota.

(A) IHC staining to detect Chi3l1 in both ileum and colon from germ-free and wildtype mice. Ctrl (wildtype mice without application of first antibody), WT (wildtype C57B/6J mice). Red arrows indicate Chi3l1-expressing cells. Scale bar, 50μm (Ctrl, Germ-free, WT) and 20μm(zoom). The number of Chi3l1-positive cells in each field of view (FOV) was analyzed. **(B)** Ileum and colon were collected from wildtype mice and stained with ChgA (green), Chi3l1(red), and nuclear DAPI (blue) in ileum and UEA-1 (green), Chi3l1(red), and nuclear DAPI (blue) in colon. Scale bar, 20μm. Ctrl (without application of first antibody), WT (wildtype C57B/6J mice). **(C)** Western blot to detect Chi3l1 protein expression in DLD-1 cells after bacteria mix infection for 12 hour. Bacteria mix are total bacteria extracted from feces of wildtype mice. **(D)** Western blot to detect Chi3l1 protein expression in DLD-1 cells after *Staphylococcus Sciuri* and *E. coli* infection for 12 hour. *Staphylococcus Sciuri* and *E. coli* are isolated from bacteria mix and verified by 16S rRNA sequencing. Three independent experimental results are showed. **(E)** Western blot to detect Chi3l1 protein expression in DLD-1 cells after treatment with heat-killed *E. coli* for 12 hour. Three independent experimental results are showed. **(F)** Western blot to detect Chi3l1 protein expression in DLD-1 cells after treatment with 100 pg/ml LPS for 12 hour. Three independent experimental results are showed. **(G)** Immunofluorescence to detect Chi3l1 protein expression in DLD-1 cells after treatment with 100pg/ml LPS for 12 hour. Scale bar, 20μm. The presence of cells in the untreated sample are annotated using white dashed lines based on the overexposure. All data above represent at least three independent experiments. Representative images are shown in A,B, n=3-4 mice/group.

Figure 2. Chi3l1 interact with bacteria via peptidoglycan.

749 **(A)** Structural comparison between Chitin and peptidoglycan. Both chitin and peptidoglycan
750 contain N-acetylglucosamine (GlcNAc) and have β-1,4-glycosidic bonds in their structures.
751 However, Chitin is purely a polysaccharide, while peptidoglycan includes a peptide component
752 that forms cross-links between chains.[30] **(B)** Gram-positive bacteria (*E.faecalis*, *S.saprophyticus*)
753 and Gram-negative bacteria (*E.coli*) were incubated with 1μg of recombinant mouse Chi3l1
754 protein(rmChi3l1), respectively. Proteins bound to indicated bacteria were precipitated by
755 centrifugation. Western blot was used to detect rmChi3l1 in Pellet, Supernatant (unbound proteins)
756 and Last Wash (last wash unbound proteins). **(C)** Insoluble Peptidoglycan (PGN) were incubated
757 with either recombinant mouse Chi3l1 protein (rmChi3l1) or Bovine serum albumin (BSA).
758 Proteins bound to PGN were precipitated by centrifugation. Silver staining was used to detect
759 rmChi3l1 in Input, Supernatant (unbound proteins), Pellet and Last Wash (last wash unbound
760 proteins). **(D)** Insoluble Peptidoglycan (PGN) were incubated with recombinant human Chi3l1
761 protein (rhChi3l1). Proteins bound to PGN were precipitated by centrifugation. Silver staining was
762 used to detect rhChi3l1 in Input, Supernatant (unbound proteins), Pellet and Last Wash (last wash
763 unbound proteins). All data above represent at least three independent experiments. **(E)** Insoluble
764 PGN or chitin was incubated with rmChi3l1. Chi3l1 bound to PGN (upper panel) and chitin
765 (lower panel) was precipitated and detected by silver staining. The supernatant represents the last
766 wash, and the pellet contains proteins precipitated by either PGN or chitin. **(F)** Relative DLD-1
767 bacterial binding preference after treatment with K12 or GlmM, a PGN synthesis-deficient mutant.
768 Colony-forming units (CFU) were counted, and GlmM CFU were normalized to 1. **(G)** Relative
769 K12 bacterial adhesion preference after DLD-1 cells were transfected without (Mock), or with
770 scramble shRNA (shCK), or with shChil1. CFU were counted, and the Mock group were
771 normalized to 1.
772
773 **Figure 3. Intestinal bacteria are disordered in IEC$^{\Delta Chil1}$ mice, especially Gram-positive**
774 **bacteria.**
775 **(A, C, D, G)** Female Villin-cre and IEC$^{\Delta Chil1}$ littermates continue to cage together after weaning
776 for 8 weeks. Microbial communities in feces and intestinal lumen were characterized by 16S
777 rRNA sequencing. n=7 or 10/group. **(A)** Alpha diversity analysis of colon contents between Villin-
778 cre and IEC$^{\Delta Chil1}$ littermates. **(B)** qPCR analysis of total bacteria in the feces and ileum, colon
779 luminal microbial communities of Villin-cre and IEC$^{\Delta Chil1}$ littermates. Values for each bacterial
780 group are expressed relative to total 16S rRNA levels. Mean ± SEM is displayed. Two-tailed,
781 unpaired student t-test was performed. *P<0.05, ns, not significant. n=5-10/group. **(C)** Principal
782 Component Analysis of weighed UniFrac distances of 16S community profiles of Villin-cre and
783 IEC$^{\Delta Chil1}$ littermates feces (binary-jaccard). **(D)** Relative abundance of Gram-positive and Gram-
784 negative bacteria in colon contents of Villin-cre and IEC$^{\Delta Chil1}$ littermates are shown. **(E)** LTA
785 (green) was detected by immunofluorescence in colon sections of Villin-cre and IEC$^{\Delta Chil1}$
786 littermates. Nuclei were detected with DAPI. Scale bar, 50μm. The average fluorescence intensity
787 in each field of view (FOV) was analyzed. **(F)** Fluorescence in situ hybridization (FISH) detection
788 of gram-positive bacteria (red) in the colon of Villin-cre and IEC$^{\Delta Chil1}$ littermates, nuclei were
789 detected with DAPI (blue). Scale bars, 50um. The average fluorescence intensity in each field of
790 view (FOV) was analyzed. **(G)** Relative abundance of Gram-positive bacteria genera in colon
791 lumen of Villin-cre and IEC$^{\Delta Chil1}$ littermates. **(H)** Female wildtype and Chil1$^{-/-}$ littermates continue
792 to cage together after weaning for 8 weeks. Microbial communities in feces were characterized by

16S rRNA sequencing. Mean ± SEM is displayed. Two-tailed, unpaired student t-test was performed. ****P<0.0001, ns, not significant. n=4 or 6/group. Representative images are shown in E, F, n= 3/4 mice/group.

Figure 4. Chi3l1 promotes the colonization of Gram-positive bacteria in intestinal mucus layer.

(A) IHC staining to detect Chi3l1 in colon mucus layer from wildtype mice. Ctrl (without application of ant-Chi3l1 antibody), WT (wildtype C57B/6J mice). Black dotted line outlines mucus layer. Scale bar, 50μm (Ctrl, WT). **(B)** Colons were collected from wildtype mice and stained with UEA-1 (green), Chi3l1(red), and nuclear DAPI (blue). Ctrl (without application of first antibody), WT (wildtype C57B/6J mice). Scale bars, 50um (Ctrl, WT) and 20μm(zoom). **(C)** Stool, ileum and colon tissues were collected from wildtype mice. Western blot was used to detect Chi3l1 expression in these samples. n=3 mice/sample. **(D)** Both luminal and mucus-associated proteins of either ileum or colon were extracted. Western blot was used to detect Chi3l1 expression in these samples. lumen (luminal proteins), mucus (mucus-associated proteins). n=3 mice/sample. **(E&F)** qPCR analysis of specific bacteria in the ileum and colon mucus microbial communities of wildtype and Chil1$^{-/-}$ littermates. **(E)** qPCR analysis of Gram-positive bacteria is shown. **(F)** qPCR analysis of Gram-positive bacteria is shown. Values for each bacterial group are expressed relative to total 16S rRNA levels. WT (wildtype C57B/6J mice). Mean ± SEM is displayed. Two-tailed, unpaired student t-test was performed. P value is as indicated in E. *P<0.05, **P<0.01, n=6-9/group. **(G)** Rectal injection of both wildtype and Chi11$^{-/-}$ mice with FDAA-labeled *E. faecalis* (a Gram-positive bacteria strain) for 4 hour. Colon sections were collected and colonization of *E.faecalis* was examined under microscope. Nuclei were stained with DAPI. Representative images are shown in A, B, G, n=3-4 mice/group.

Figure 5. Disordered intestinal bacteria in IEC$^{\Delta Chil1}$ mice contribute to IBD.

(A) *Chil1* mRNA relative expression in colon tissues of patients without gut disease (controls, n=35) or with Crohn's disease (CD, n=40), ulcerative colitis (UC, n=40), (GEO Datasets: SRP303290), Mann-Whitney test was performed. *P < 0.05; ***P < 0.001. **(B)** Schematic model of the experimental design. Both Villin-cre and IEC$^{\Delta Chil1}$ littermates were fed with 2% DSS in drinking water to induce colitis. **(C)** Weight change of Villin-cre and IEC$^{\Delta Chil1}$ littermates during DSS feeding. Weight change (%) = Current weight/Initial weight. P values are as indicated. **(D)** Representative colonic length from Normal and DSS-treated Villin-cre and IEC$^{\Delta Chil1}$ littermates (left) and the statistics of colonic length (right) (**P < 0.01; ***P < 0.001; ****P < 0.0001, ns, not significant). **(E)** H&E staining of mice colon from Normal and DSS-treated Villin-cre and IEC$^{\Delta Chil1}$ littermates. The inflamed areas are outlined by white dotted line, Scale bars=100um. **(F)** Schematic of the experimental design. First, antibiotics were used to eliminate gut microbiota for 10 days, and then either fecal microbiota from Villin-cre mice (FMT) or *Lactobacillus reuteri* were transplanted back *to* IEC$^{\Delta Chil1}$ mice orally every day for 2 weeks. Finally, colitis mouse model was constructed by 2% DSS feeding in drinking water for another 7 days. **(G-I)** Villin-cre and IEC$^{\Delta Chil1}$ were only fed with 2% DSS in drinking water for 7days. IEC$^{\Delta Chil1}$+FMT(Villin-cre), and IEC$^{\Delta Chil1}$+*Lactobacillus* were constructed as described in F. **(G)** Weight change of Villin-cre, IEC$^{\Delta Chil1}$, IEC$^{\Delta Chil1}$+FMT(Villin-cre), and IEC$^{\Delta Chil1}$+*Lactobacillus* mice during DSS feeding. **(H)** Representative colonic length from Villin-cre, IEC$^{\Delta Chil1}$, IEC$^{\Delta Chil1}$+FMT(Villin-cre), and

IEC$^{\Delta Chil1}$+*Lactobacillus* mice (left) and the statistics of colonic length (right). Mean ± SEM is displayed in G, H. one-way ANOVA was performed. P value is as indicated. *P<0.05, ns, not significant, n=3-6/group. **(I)** H&E staining of mice colon from Villin-cre, IEC$^{\Delta Chil1}$, IEC$^{\Delta Chil1}$+FMT(Villin-cre), and IEC$^{\Delta Chil1}$+*Lactobacillus* mice after DSS treatment. The inflamed area is outlined by black dotted line, Scale bars=100um. Representative images are shown in C, E, H, I, n=3-6 mice/group.

Figure 6. A schematic working model. Intestinal epithelial cells are stimulated by the gut microbiota to express Chi3l1. Once expressed, Chi3l1 is secreted into the mucus layer where it interacts with the gut microbiota, specifically through a component of bacterial cell walls called peptidoglycan. This interaction between Chi3l1 and bacteria is beneficial for the colonization of bacteria in the mucus, particularly for gram-positive bacteria like *Lactobacillus*. Moreover, a deficiency of Chi3l1 leads to an imbalance in the gut microbiota, which exacerbates colitis induced by dextran sodium sulfate (DSS).

Figure 1

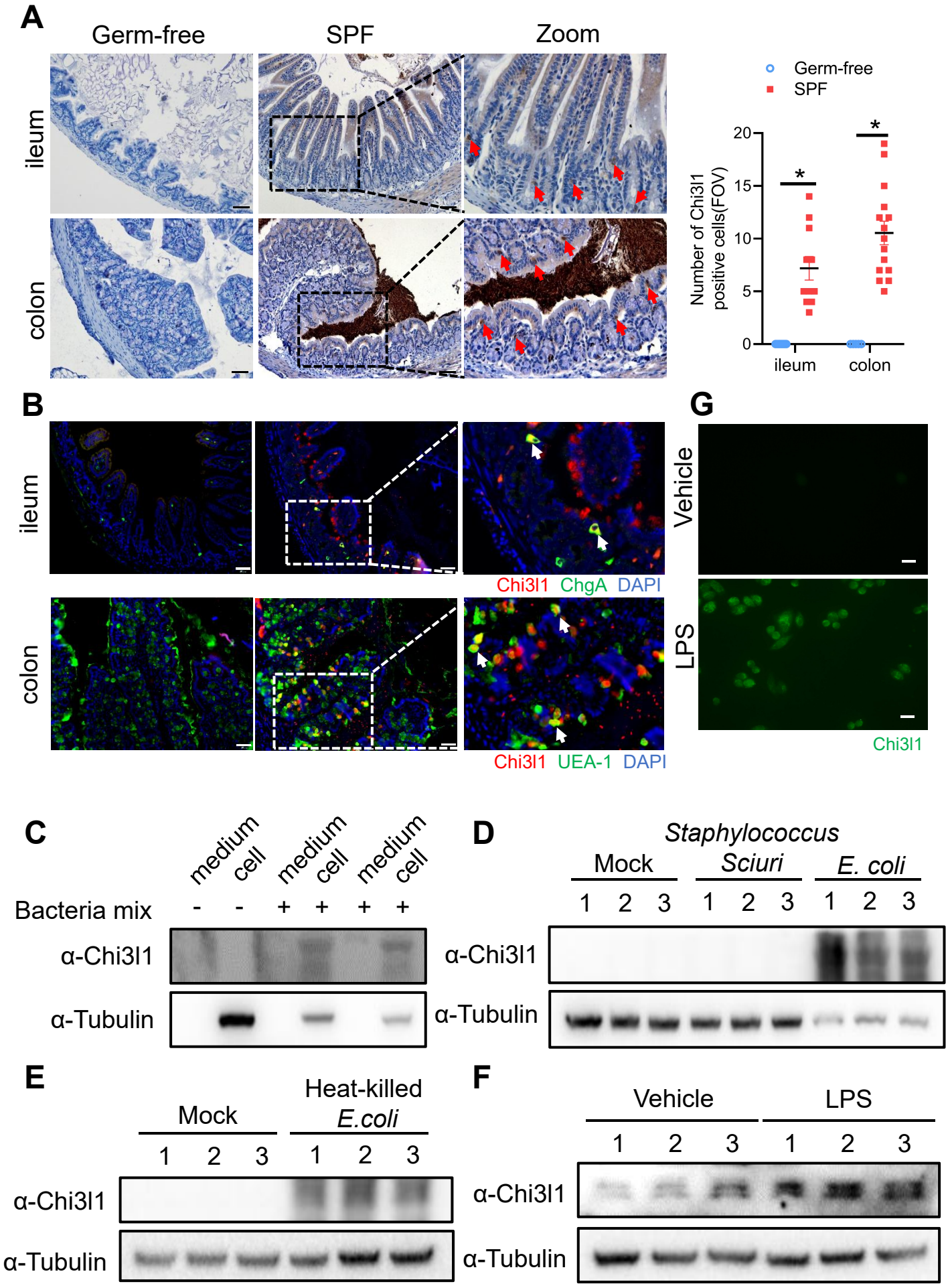
A
Germ-free
SPF
Zoom
ileum
colon
Germ-free
SPF
Number of Chi3l1 positive cells(FOV)
20
15
10
5
0
*
*
ileum
colon
B
ileum
colon
Chi3l1 ChgA DAPI
Chi3l1 UEA-1 DAPI
G
Vehicle
LPS
Chi3l1
C
medium
cell
medium
cell
medium
cell
Bacteria mix
- - + + + +
α-Chi3l1
α-Tubulin
D
Staphylococcus
Mock
Sciuri
E. coli
1 2 3 1 2 3 1 2 3
α-Chi3l1
α-Tubulin
E
Mock
Heat-killed
E.coli
1 2 3 1 2 3
α-Chi3l1
α-Tubulin
F
Vehicle
LPS
1 2 3 1 2 3
α-Chi3l1
α-Tubulin

Figure 2

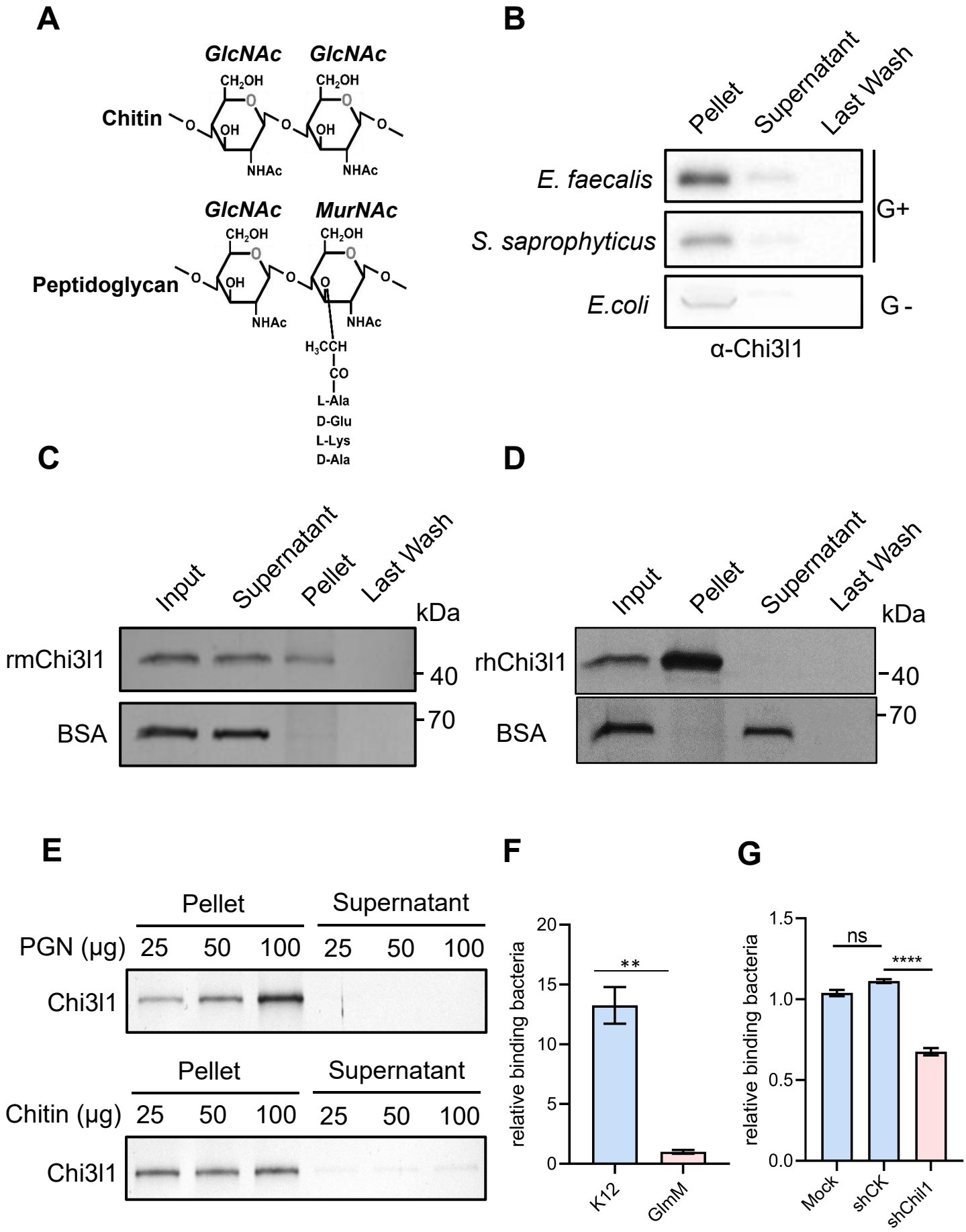
A
GlcNAc
GlcNAc
Chitin
CH2OH
OH
NHAc
GlcNAc
MurNAc
Peptidoglycan
H3CCH
CO
L-Ala
D-Glu
L-Lys
D-Ala
B
Pellet
Supernatant
Last Wash
E. faecalis
S. saprophyticus
E.coli
G+
G -
α-Chi3l1
C
Input
Supernatant
Pellet
Last Wash
kDa
rmChi3l1
BSA
40
70
D
Input
Pellet
Supernatant
Last Wash
kDa
rhChi3l1
BSA
40
70
E
Pellet
Supernatant
PGN (μg) 25 50 100 25 50 100
Chi3l1
Pellet
Supernatant
Chitin (μg) 25 50 100 25 50 100
Chi3l1
F
relative binding bacteria
20
15
10
5
0
**
K12
GlmM
G
relative binding bacteria
1.5
1.0
0.5
0.0
ns
****
Mock
shCK
shChil1

Figure 3

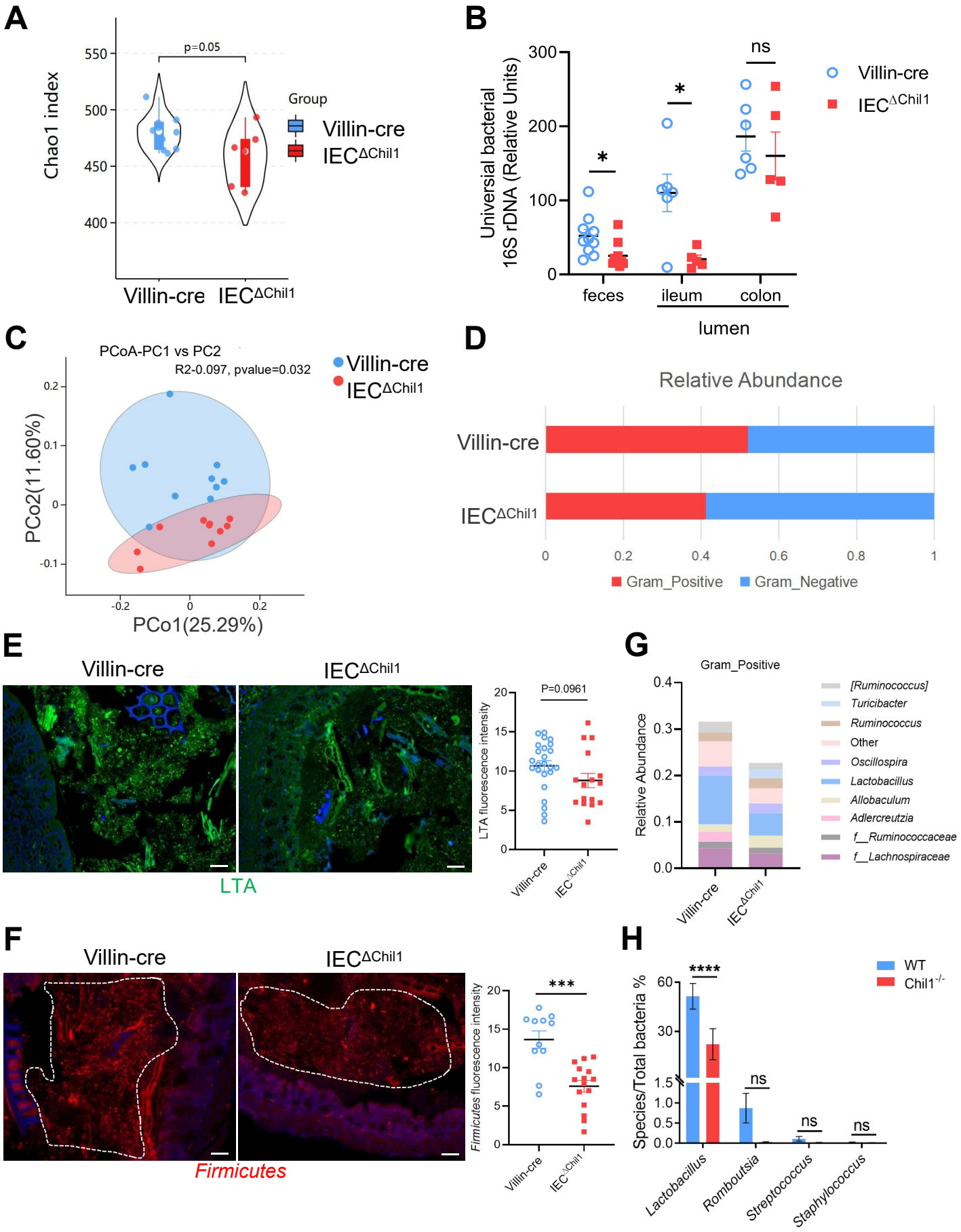
A
Chao1 index
p=0.05
550
500
450
400
Group
Villin-cre
IECΔChil1
Villin-cre
IECΔChil1
B
Universal bacterial 16S rDNA (Relative Units)
300
200
100
0
*
*
ns
feces
ileum
colon
lumen
Villin-cre
IECΔChil1
C
PCoA-PC1 vs PC2
R2-0.097, pvalue=0.032
PCo2(11.60%)
PCo1(25.29%)
0.2
0.1
0
-0.1
-0.2
0
0.2
Villin-cre
IECΔChil1
D
Relative Abundance
Villin-cre
IECΔChil1
0
0.2
0.4
0.6
0.8
1
Gram_Positive
Gram_Negative
E
Villin-cre
IECΔChil1
LTA
P=0.0961
LTA fluorescence intensity
20
15
10
5
0
Villin-cre
IECΔChil1
G
Gram_Positive
Relative Abundance
0.4
0.3
0.2
0.1
0.0
Villin-cre
IECΔChil1
[Ruminococcus]
Turicibacter
Ruminococcus
Other
Oscillospira
Lactobacillus
Allobaculum
Adlercreutzia
f__Ruminococcaceae
f__Lachnospiraceae
F
Villin-cre
IECΔChil1
Firmicutes
***
Firmicutes fluorescence intensity
20
15
10
5
0
Villin-cre
IECΔChil1
H
WT
Chil1-/-
Species/Total bacteria %
****
60
30
1.5
1.0
0.5
0.0
ns
ns
ns
Lactobacillus
Romboutsia
Streptococcus
Staphylococcus

Figure 4

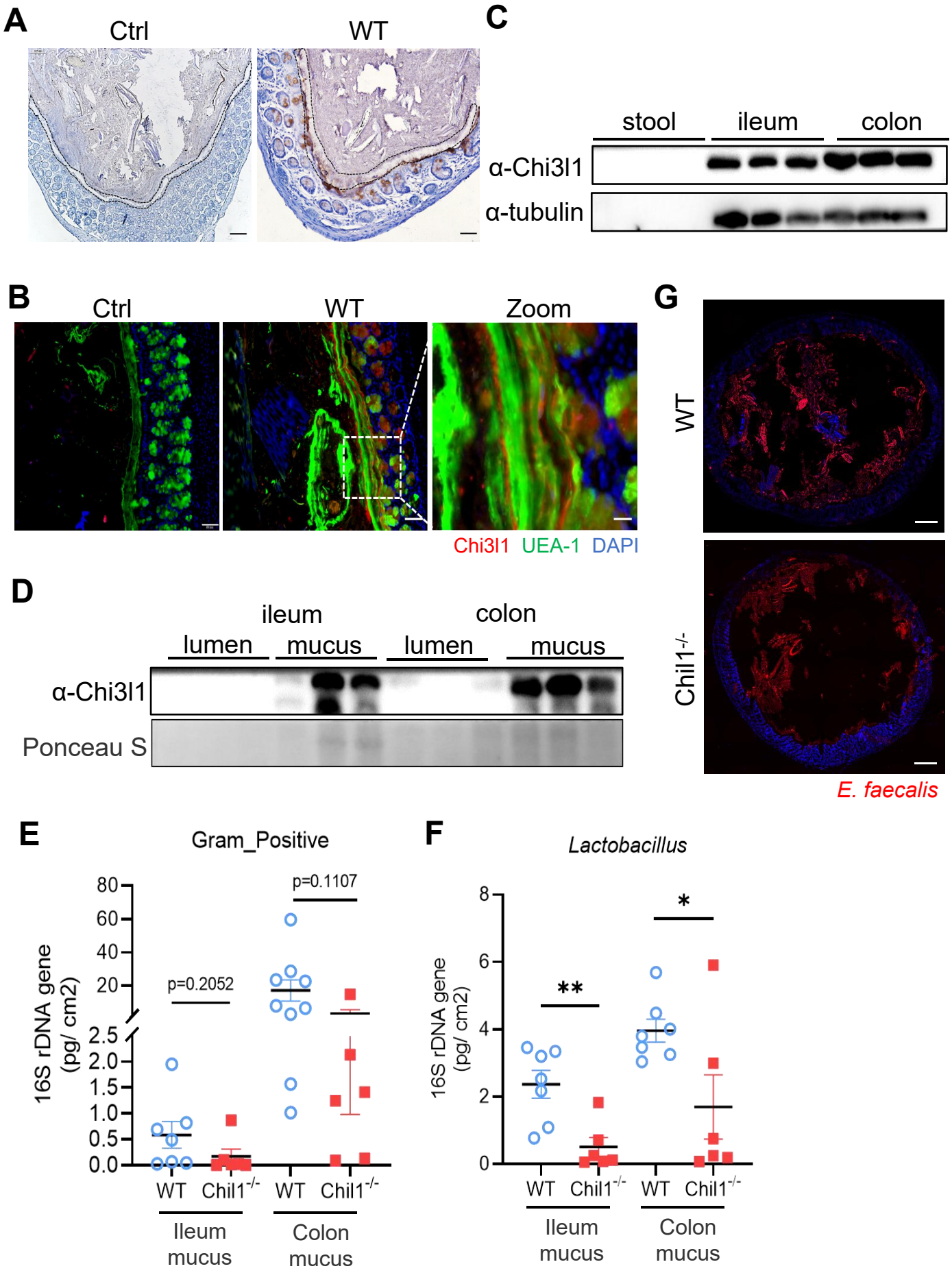
A
Ctrl
WT
C
stool
ileum
colon
α-Chi3l1
α-tubulin
B
Ctrl
WT
Zoom
Chi3l1 UEA-1 DAPI
G
WT
Chil1-/-
E. faecalis
D
ileum
colon
lumen
mucus
lumen
mucus
α-Chi3l1
Ponceau S
E
Gram_Positive
16S rDNA gene (pg/ cm2)
p=0.2052
p=0.1107
WT
Chil1-/-
WT
Chil1-/-
Ileum mucus
Colon mucus
F
Lactobacillus
16S rDNA gene (pg/ cm2)
**
*
WT
Chil1-/-
WT
Chil1-/-
Ileum mucus
Colon mucus

Figure 5

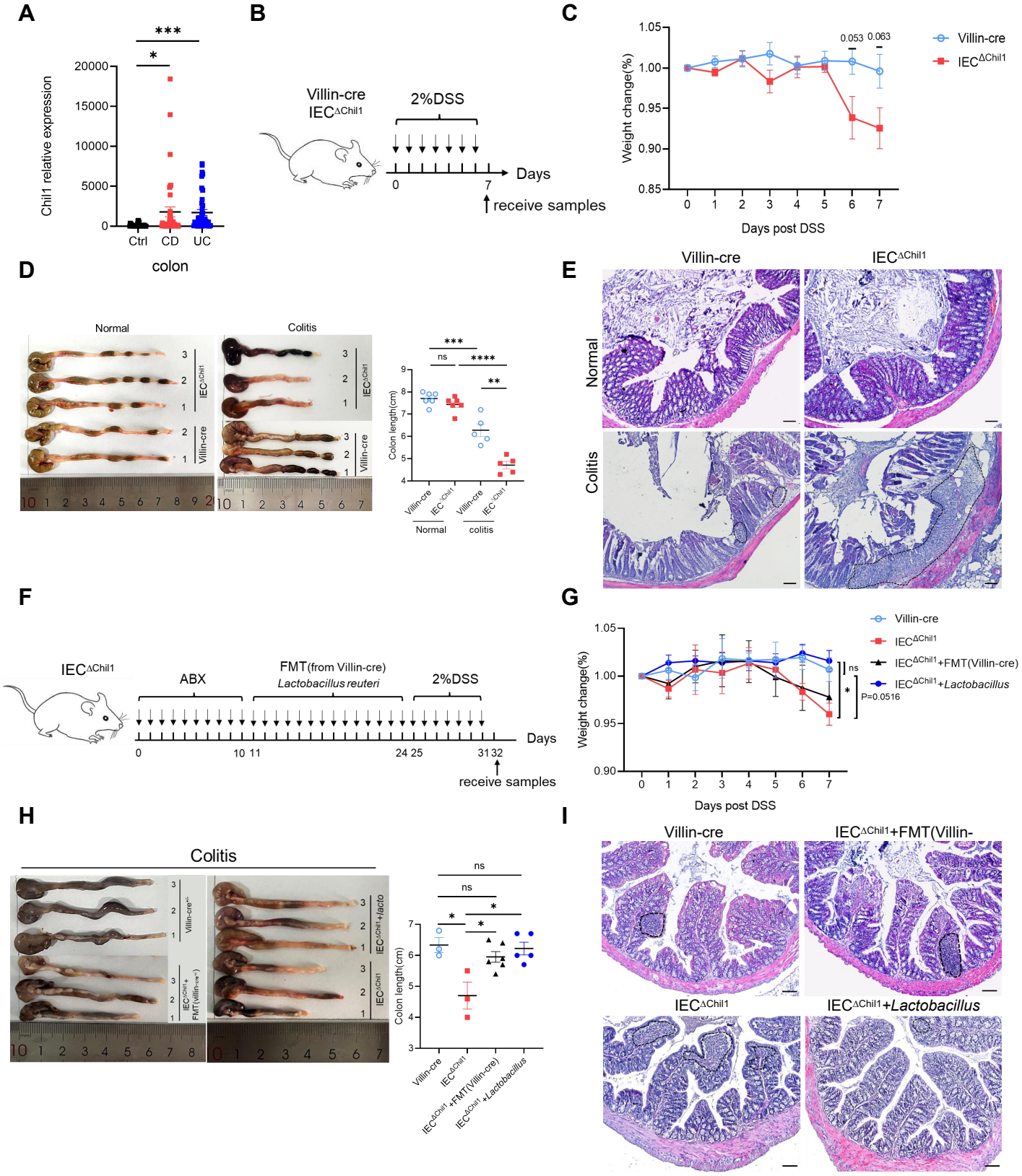
A
Chil1 relative expression
Ctrl
CD
UC
colon
B
Villin-cre
IECΔChil1
2%DSS
Days
receive samples
C
Weight change(%)
Days post DSS
Villin-cre
IECΔChil1
0.053
0.063
D
Normal
Colitis
Colon length(cm)
E
Villin-cre
IECΔChil1
Normal
Colitis
F
IECΔChil1
ABX
FMT(from Villin-cre)
Lactobacillus reuteri
2%DSS
Days
receive samples
G
Weight change(%)
Days post DSS
Villin-cre
IECΔChil1
IECΔChil1+FMT(Villin-cre)
IECΔChil1+Lactobacillus
P=0.0516
H
Colitis
Colon length(cm)
I
Villin-cre
IECΔChil1+FMT(Villin-
IECΔChil1
IECΔChil1+Lactobacillus

Figure 6

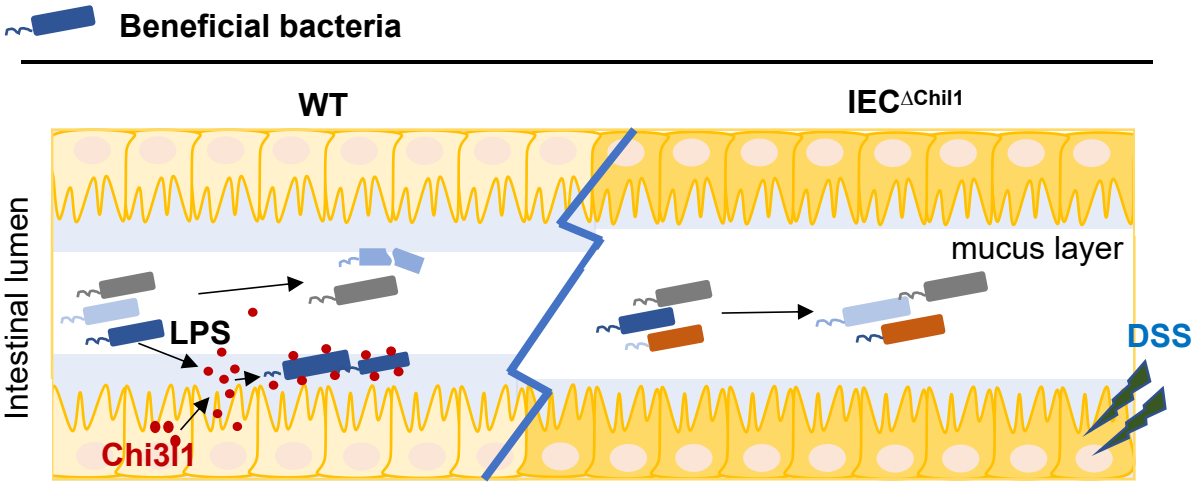
Beneficial bacteria
WT
IEC$^{\Delta Chil1}$
Intestinal lumen
mucus layer
LPS
DSS
Chi3l1